2008

Electrochemical Deposition of Porous Co(OH)2 Nanoflake Films on Stainless Steel Mesh for Flexible Supercapacitors

Shulei Chou
Institute for Superconducting and Electronic Materials, shulei@uow.edu.au

Jiazhao Wang
Institute for Superconducting and Electronic Materials, jiazhao@uow.edu.au

Hua-Kun Liu
Institute for Superconducting and Electronic Materials, hua@uow.edu.au

S. X. Dou
Institute for Superconducting and Electronic Materials, shi@uow.edu.au

Journal of The Electrochemical Society, **155** (12) A926-A929 (2008)
0013-4651/2008/155(12)/A926/4/$23.00 © The Electrochemical Society

Electrochemical Deposition of Porous $Co(OH)_2$ Nanoflake Films on Stainless Steel Mesh for Flexible Supercapacitors

Shu-Lei Chou,[a,b,*,z] Jia-Zhao Wang,[a,b] Hua-Kun Liu,[a,b,] and Shi-Xue Dou[a]**

[a]*Institute for Superconducting and Electronic Materials and* [b]*ARC Center of Excellence for Electromaterials Science, University of Wollongong, Wollongong, NSW 2522, Australia*

Flexible porous $Co(OH)_2$ nanoflake films were prepared by galvanostatic electrodeposition on lightweight and inexpensive stainless steel mesh. The as-prepared porous $Co(OH)_2$ nanoflake films were characterized by X-ray diffraction, thermogravimetric analysis, and scanning electron microscopy. Electrochemical tests including cyclic voltammetry, constant current charge–discharge, and electrochemical impedance spectroscopy were also used to investigate the electrochemical performance. The results show that the highest capacitance is 609.4 F g^{-1}, the specific capacitance decreases by less than 5% as the mass loading of $Co(OH)_2$ increases by more than 340%, and the specific capacitance only decreases by less than 15% when the current densities increase up to 10 times, indicating the good high-rate performance. The electrochemically active specific surface area of the annealed porous $Co(OH)_2$ nanoflake films remained virtually unchanged after 3000 cycles, showing the stability of the microstructure.
 [DOI: 10.1149/1.2988739]

Manuscript submitted June 30, 2008; revised manuscript received August 18, 2008. Published October 9, 2008.

In recent years, the rapid development of portable devices (e.g., mobile phones, computers, and special medical devices) has created an urgent requirement for high-performance supercapacitors, which should have not only a high capacitance, but also good mechanical properties (lightweight and even flexibility).[1-3] Stainless steel mesh, which is lightweight, inexpensive, and has good mechanical properties, has been used as an electrode substrate for batteries or supercapacitors.[4,5] From the active materials point of view, considering the low capacitance of carbon (in electrical double-layer capacitors), researchers have paid much more attention to metal oxides/hydroxides (in pseudocapacitors), which show higher specific capacitance, because redox reactions can contribute extra capacitance.[6,7] Among the metal oxides/hydroxides, RuO_2 shows the highest capacitance and ideal capacitor performance, but the high cost is the big hindrance for commercial usage.[8-11] Cobalt hydroxide [$Co(OH)_2$], an important electrode material with a lower cost, has become increasingly attractive for applications in supercapacitors.[12-19] Furthermore, nanostructured or porous materials, usually with a high surface area, have demonstrated great advantages as electrode materials, including shortening the diffusion length of ions and increasing the contact surface area with the electrolyte.[20-22] To date, Li's group has synthesized mesoporous $Co(OH)_2$ with a high specific capacitance of 1492 F g^{-1} by casting it into pores of molecular sieve templates.[20,21] Recently, Gupta et al. used potentiostatic electrochemical deposition to prepare $Co(OH)_2$ nanosheets which showed specific capacitances up to 860 F g^{-1}.[22] However, there has been no report on the preparation of a totally flexible electrode for supercapacitors with porous $Co(OH)_2$ nanostructures as active materials. Here, we used galvanostatic electrodeposition to prepare porous $Co(OH)_2$ nanostructured films on lightweight and inexpensive stainless steel mesh, and the morphologies of the $Co(OH)_2$ could be easily controlled via simple adjustment of the current density.[23] The other advantage is that the as-prepared flexible electrode could be directly used to assemble totally flexible supercapacitors using a solid-state electrolyte.[2,3]

Experimental

The porous $Co(OH)_2$ nanoflake thin films were electrodeposited at room temperature in a two-electrode system onto stainless steel mesh (Metal Mesh Pty Ltd., Australia). Pt foil was used as the counter electrode. The electrolyte was 0.025 M $Co(NO_3)_2$ solution, in accordance with our recent investigation.[23] Typically, the porous $Co(OH)_2$ nanoflake thin films were prepared by using galvanostatic electrochemical deposition at a current density of 1 mA cm^{-2} for 3, 10, and 20 min with $Co(OH)_2$ loading masses of 0.14, 0.39, and 0.62 mg cm^{-2}, respectively. The as-obtained porous $Co(OH)_2$ nanoflake films on stainless steel mesh were washed with deionized water three times, allowed to dry in air, and then annealed at 150°C in air for 2 h.

The morphology and microstructure of the as-prepared porous $Co(OH)_2$ nanoflake films were characterized by X-ray diffraction (XRD; GBC MMA 017), scanning electron microscopy (SEM; JEOL JEM-3000), and thermogravimetric analysis (TGA; TA 2000 thermoanalyzer). Electrochemical measurements were tested in a three-electrode electrochemical cell, including charge–discharge (Neware battery test system), and cyclic voltammetry (CV) and electrochemical impedance spectroscopy (EIS) (CHI 660 electrochemistry workstation). The electrochemical cell was composed of as-prepared porous $Co(OH)_2$ nanoflakes on stainless steel mesh as the working electrode, a Pt foil sheet (4 cm^2) as the counter electrode, a standard calomel electrode (SCE) as the reference electrode, and 1 M KOH solution as the electrolyte.

Results and Discussion

Figure 1 shows XRD patterns, TGA results, and SEM images. It can be observed in Fig. 1A that the XRD patterns show broad peaks between 15 and 40°, indicating the amorphous crystal structure of $Co(OH)_2$, regardless of whether the sample was on or off substrate. The TGA curves (shown in Fig. 1B) mainly demonstrated two stages. Below 175°C, the weight loss is due to the evaporation of absorbed water, as the XRD pattern at 150°C of the $Co(OH)_2$ still shows an amorphous crystal structure (Fig. 1A and B). Between 175 and 400°C, weight loss occurs because the $Co(OH)_2$ is decomposing and oxidizing to Co_3O_4.[24] It has also been reported that $Co(OH)_2$ annealed at 150°C in air for 3 h showed a higher surface area and higher capacitance,[12] so the as-prepared $Co(OH)_2$ samples on stainless steel mesh were all annealed at 150°C for 3 h in air for further characterizations in order to improve the performance. SEM images of the nanoflake electrode are shown in Fig. 1C-E. Figure 1C reveals that the $Co(OH)_2$ is homogeneously coated on the wires of the stainless steel mesh. The inset of Fig. 1C contains a photograph of $Co(OH)_2$-loaded stainless steel mesh between two fingers, showing the good flexibility of the $Co(OH)_2$ on stainless steel mesh electrode. Figure 1D, an enlargement of Fig. 1C, shows that the coating has a porous structure. The higher resolution SEM image in Fig. 1E shows that the $Co(OH)_2$ has a flowerlike porous nanostructure, which is formed by a network of nanoflakes 20–30 nm thick.

Figure 2 displays the electrochemical test results. Cyclic voltam-

* Electrochemical Society Student Member.
** Electrochemical Society Active Member.
z E-mail: sc478@uow.edu.au

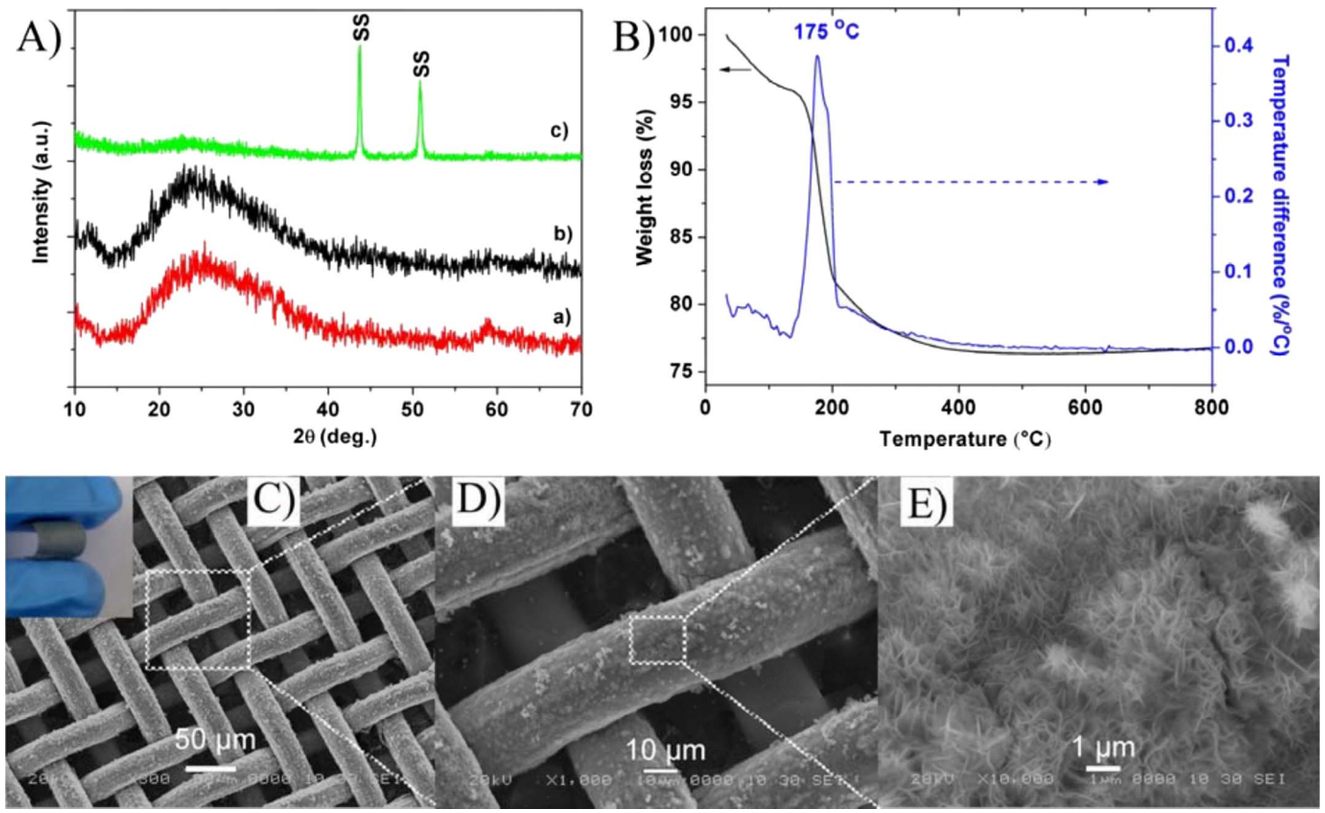

Figure 1. (Color online) (A) XRD patterns of $Co(OH)_2$ (a) off the stainless steel mesh (b), off the mesh and annealed at 150°C, and (c) on the stainless steel mesh, (B) TGA curves of $Co(OH)_2$ off the stainless steel mesh from 30 to 800°C in air, (C), (D) SEM images with low magnifications and (E) high magnification of porous $Co(OH)_2$ nanostructures on stainless steel mesh. The inset in (C) is a photograph of $Co(OH)_2$-loaded stainless steel mesh between two fingers.

mograms of electrodeposited porous $Co(OH)_2$ nanoflake thin films, collected after annealing at 150°C for 3 h in air, at scan rates of 5, 10, 20, and 50 mV s^{-1} are shown in Fig. 2a. Quasi-reversible redox peaks are observed in the voltage ranges from −0.05 to 0 and 0.05–0.15 V, which may be briefly described by Eq. 1 [25]

$$Co(OH)_2 + OH^- \Leftrightarrow CoOOH + H_2O + e^- \quad [1]$$

The quasi-reversible redox reaction shows that the porous $Co(OH)_2$ nanoflake thin films can be used as electrode materials in redox supercapacitors. As the scan rate increases, the overall shape of the CV curves is still maintained, indicating good high-rate performance. The specific capacitances calculated from the CV curves are 609.9, 563.5, 507.5, and 427.4 F g^{-1} for scan rates of 5, 10, 20, and 50 mV s^{-1}, respectively. Different charge–discharge current densities were used in investigating the capacitance behavior of porous $Co(OH)_2$ nanoflake films with different loading rate, as shown in Fig. 2b and c. Figure 2b displays almost symmetrical charge and discharge curves at different current densities, indicating the good coulombic efficiency of the porous $Co(OH)_2$ nanoflakes as supercapacitors. The specific capacitances with different $Co(OH)_2$ loadings, as calculated from the charge–discharge curves, are shown in Fig. 2c. The highest specific capacitance is 562 F g^{-1} at a current density of 0.1 mA g^{-1} for the smallest $Co(OH)_2$ mass loading of 0.14 mg cm^{-2}. The specific capacitance decreases by less than 5% as the mass loading of $Co(OH)_2$ increases by more than 340% from 0.14 to 0.62 mg cm^{-2}. The specific capacitance only decreases by less than 15% when the current densities increase up to 10 times from 714 to 7143 mA g^{-1}, indicating the good high-rate performance. These results might be due to the porous nanostructure, which allows for the easy penetration of the electrolyte and shortens the diffusion length of ions.

Figure 2d displays the effect of cycling on the electrode composed of annealed porous $Co(OH)_2$ nanoflakes on stainless steel mesh for up to 3000 cycles. There is only 19% specific capacitance loss after 3000 cycles, which shows the long-term electrochemical stability. After 3000 cycles, the specific capacitance of the porous $Co(OH)_2$ nanoflake electrode is 364 F g^{-1}, which is still higher than that of carbon-based materials.[26] Figure 2e shows cyclic voltammograms of porous $Co(OH)_2$ nanoflake films after 50 cycles and after 3000 cycles at a scan rate of 5 mV s^{-1}. The quasi-reversible redox couple of $R1 \leftrightarrow O1$ is due to the reaction listed before in Eq. 1. The quasi-reversible redox couples of $R2 \leftrightarrow O2$ and $R3 \leftrightarrow O3$ are due to Eq. 2 and 3, respectively.[27] The loss of the capacitance is because the $Co(OH)_2$ is gradually transformed from $Co(OH)_2$ to Co_3O_4 during cycling.[16] $O4$ is due to the oxygen evolution

$$CoOOH + OH^- \Leftrightarrow CoO_2 + H_2O + e^- \quad [2]$$

$$Co_3O_4 + 4OH^- \Leftrightarrow 3CoO_2 + 2H_2O + e^- \quad [3]$$

Typical impedance spectra of porous $Co(OH)_2$ nanoflake films are shown in Fig. 3. Figure 3a displays the whole range of frequencies from 10 kHz to 100 mHz at bias potentials of 0.06, 0.2, and 0.4 V (vs SCE). It can be seen that porous $Co(OH)_2$ nanoflake electrode shows almost a straight vertical line along the imaginary axis Z'', indicating the lower diffusive resistance of the electrolyte in porous electrode and the proton diffusion in the host materials at the lower frequencies. This might be caused by the porous nanostructures, which have uniform pores, allowing better access to the elec-

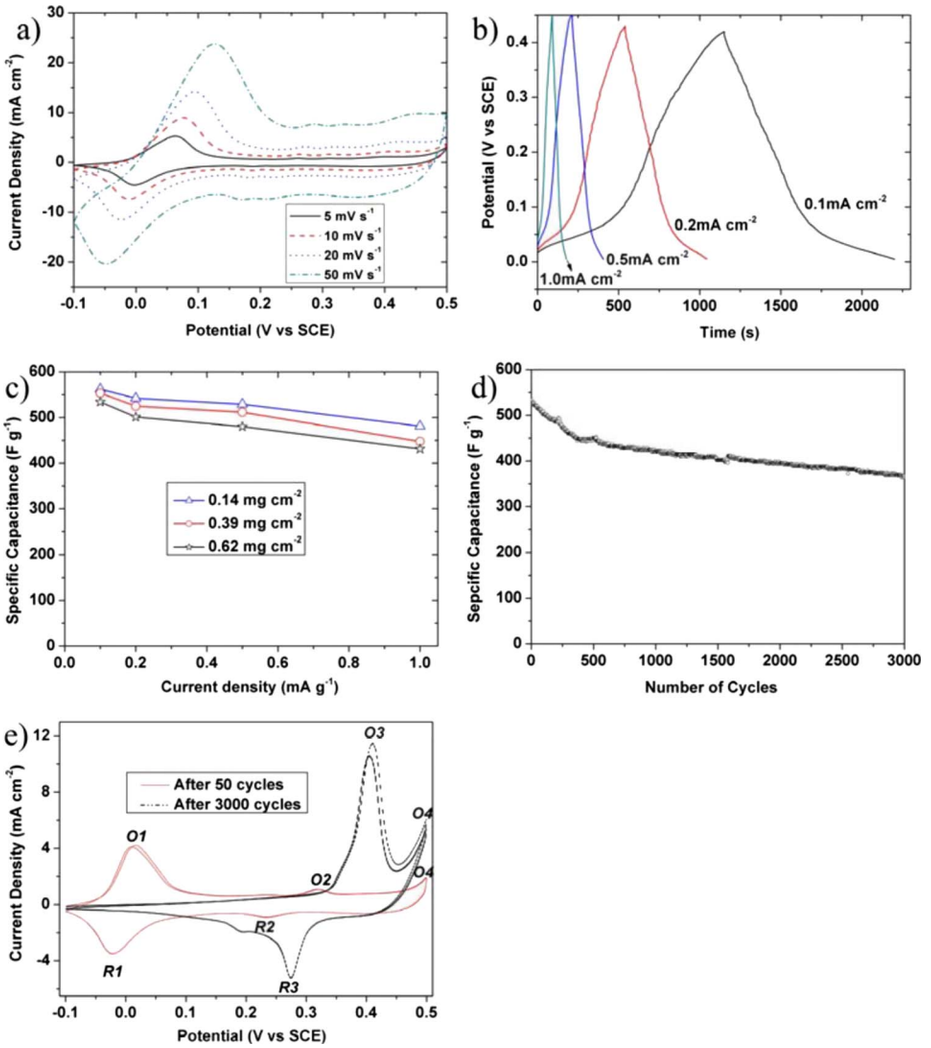

Figure 2. (Color online) (a) Cyclic voltammograms of as-annealed porous $Co(OH)_2$ nanoflake films at different scan rates with a $Co(OH)_2$ mass loading of 0.39 mg cm^{-2}, (b) Charge–discharge curves of as-annealed porous $Co(OH)_2$ nanoflakes on stainless steel mesh with mass loading of 0.39 mg cm^{-2} at different current densities, (c) Specific capacitance vs current density with different $Co(OH)_2$ mass loading of 0.14, 0.39, and 0.62 mg cm^{-2}, (d) Cycle life of the as-annealed porous $Co(OH)_2$ nanoflake films at a current density of 1 mA cm^{-2} with a $Co(OH)_2$ mass loading of 0.39 mg cm^{-2}, (e) Cyclic voltammograms of as-annealed porous $Co(OH)_2$ nanoflake films after 50 cycles and after 3000 cycles at a scan rate of 5 mV s^{-1}. The electrolyte is 1 M KOH solution.

trolyte, and thus increased electrochemical activity. The inset of Fig. 3a is an enlargement of the high-frequency range. The intercepts on the real axis Z' could be considered as the combination resistance including the ionic resistance of electrolyte, intrinsic resistance of active materials, and contact resistance at the active material/current collector interface.[28,29] The combination resistance ($\sim$4.5 Ω cm^{-2}) is higher than the results previously reported (0.1 Ω cm^{-2}).[22] This may be due to the contact resistance of the stainless steel wires which form the stainless steel mesh. This might also be the reason why our capacitance is lower than the results reported previously, though the crystal structure is different.[20-22] The semicircle in the high-frequency range is associated with the surface properties of the porous electrode and corresponds to the charge-transfer resistance. The charge-transfer resistances of porous $Co(OH)_2$ nanoflake film are 1.8, 0.5, and 0.2 Ω cm^{-2} at bias potentials of 0.06, 0.2, and 0.4 V (vs SCE), respectively. Admittance plots shown in Fig. 3b display the knee frequency, which is a very important parameter related to the high-rate performance of supercapacitors. The knee frequency varies from 0.12 to 1.5 kHz when the bias potential is varied from 0.06 to 0.4 V. The frequency for a phase angle of $-45°$, also representing the power performance of the electrode, is around 0.2–0.8 Hz when the bias potential is varied from 0.2 to 0.8 V, as shown in Fig. 3c. The above analyses reveal the good performance of annealed porous $Co(OH)_2$ nanoflake films on stainless steel mesh as a flexible electrode for supercapacitors.

The electrochemically active specific surface area [$S_E(m^2\ g^{-1})$] could be calculated from the equation $S_E = C'_d/C_d$, where C_d is the constant double-layer capacitance, with a value around 20 μF cm^{-2}, and C'_d (F g^{-1}) is the tested specific capacitance of the double layer.[30,31] Because there is no electrochemical reaction at -0.2 V vs SCE, C'_d could be calculated from the equation $C'_d = -1/2\pi mfZ''$, where m (g) is the mass of the active materials, f (Hz) is the frequency in the low-frequency range, and Z'' (Ω cm^{-2}) is the imaginary impedance.[23] The electrochemically active specific surface areas are 62.7 and 59.2 m^2 g^{-1} before cycling and after 3000 cycles, respectively, indicating that the microstructure of $Co(OH)_2$ could be maintained beyond 3000 cycles, which may be the reason for the long cycle life. Further work using this kind of flexible electrode and solid-state electrolyte to assemble totally flexible supercapacitors is ongoing.

Conclusions

Flexible porous $Co(OH)_2$ nanoflake films on stainless steel mesh were synthesized by simple galvanostatic electrochemical deposition at a current density of 1 mA cm^{-2} in 0.025 M $Co(NO_3)_2$ electrolyte. The electrochemical measurements demonstrated that the annealed porous $Co(OH)_2$ nanoflake electrode can be directly used for electrochemical supercapacitors, showing a capacitance as high as 609.9 F g^{-1} in 1 M KOH, as calculated from the CV curves at a

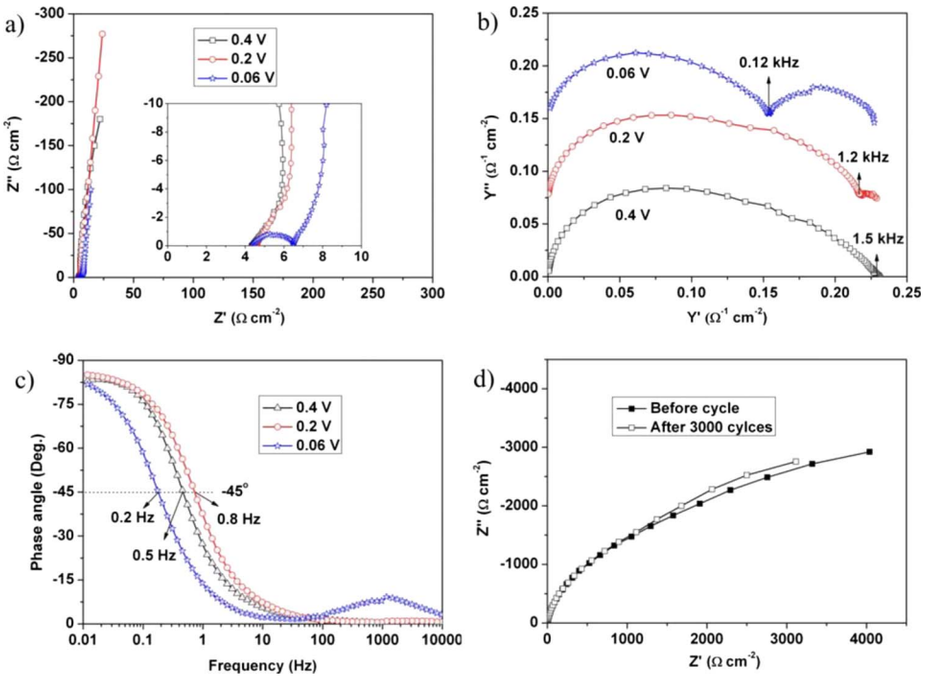

Figure 3. (Color online) (a) Nyquist impedance spectra for as-annealed porous $Co(OH)_2$ nanoflake electrode, with the inset showing an enlargement of the high-frequency region, (b) admittance plots of the nanoflake electrode, and (c) frequency dependence of the phase angle. The bias potential in (a), (b), and (c) is varied from 0.06 to 0.4 V (vs SCE). (d) Nyquist impedance spectra for porous $Co(OH)_2$ nanoflake electrode before and after 3000 cycles at −0.2 V (vs SCE). The frequency range is between 10 kHz and 10 mHz. The electrolyte for the electrochemical analyses is 1.0 M KOH.

scan rate of 5 mV s^{-1}. The electrode also showed long-term electrochemical stability up to 3000 cycles and a good high-rate performance for both thinner and thicker films. EIS made it clear that the electrochemically active specific surface area of the annealed porous $Co(OH)_2$ nanoflake films remained virtually unchanged after 3000 cycles, showing the stability of the microstructure. The capacitance loss that did occur could be attributed to the transformation from $Co(OH)_2$ to Co_3O_4. The flexible porous $Co(OH)_2$ nanoflake films could be suitable for use as the electrode for the next generation of flexible supercapacitors.

Acknowledgments

Financial support provided by the Australian Research Council (ARC) through ARC Centre of Excellence funding (CE0561616) is gratefully acknowledged. The authors thank Dr. T. Silver at the University of Wollongong for critical reading of the manuscript.

University of Wollongong assisted in meeting the publication costs of this article.

References

1. D. N. Futaba, K. Hata, T. Yamada, T. Hiraoka, Y. Hayamizu, Y. Kakudate, O. Tanaike, H. Hatori, M. Yumura, and S. Iijima, *Nature Mater.*, **5**, 987 (2006).
2. W. Sugimoto, K. Yokoshima, K. Ohuchi, Y. Murakami, and Y. Takasu, *J. Electrochem. Soc.*, **153**, A255 (2006).
3. V. L. Pushparaj, M. M. Shaijumon, A. Kumar, S. Murugesan, L. Ci, R. Vajtai, R. J. Linhardt, O. Nalamasu, and P. M. Ajayan, *Proc. Natl. Acad. Sci. U.S.A.*, **104**, 13574 (2007).
4. K. S. Park, S. B. Schougaard, and J. B. Goodenough, *Adv. Mater. (Weinheim, Ger.)*, **19**, 848 (2007); J. Wang, C. O. Too, D. Zhou, and G. G. Wallace, *J. Power Sources*, **140**, 162 (2005).
5. C. C. Hu and W. C. Chen, *Electrochim. Acta*, **49**, 3469 (2004).
6. S. Sarangapani, B. V. Tilak, and C. P. Chen, *J. Electrochem. Soc.*, **143**, 3791 (1996).
7. B. E. Conway, *Electrochemical Supercapacitors: Scientific Fundamentals and Technological Applications*, Plenum Press, New York (1999).
8. J. P. Zheng, P. J. Cygan, and T. R. Jow, *J. Electrochem. Soc.*, **142**, 2699 (1995).
9. C. C. Hu and W. C. Chen, *Electrochim. Acta*, **49**, 3469 (2004).
10. I. H. Kim, J. H. Kim, and K. B. Kim, *Electrochem. Solid-State Lett.*, **8**, A369 (2005).
11. C. C. Hu, K. H. Chang, M. C. Lin, and Y. T. Wu, *Nano Lett.*, **6**, 2690 (2006).
12. C. Lin, J. A. Ritter, and B. N. Popov, *J. Electrochem. Soc.*, **145**, 4097 (1998).
13. P. Elumalai, H. N. Vasan, and N. Munichandraiah, *J. Power Sources*, **93**, 201 (2001).
14. C. C. Hu and C. Y. Cheng, *Electrochem. Solid-State Lett.*, **5**, A43 (2002).
15. V. Srinivasan and J. W. Weidner, *J. Power Sources*, **108**, 15 (2002).
16. M. L. Zhang and Z. X. Liu, *Chin. J. Inorg. Chem.*, **18**, 513 (2002).
17. V. R. Shinde, S. B. Mahadik, T. P. Gujar, and C. D. Lokhande, *Appl. Surf. Sci.*, **252**, 7487 (2006).
18. V. Gupta, S. Gupta, and N. Miura, *J. Power Sources*, **177**, 685 (2008).
19. C. C. Hu and T. Y. Hsu, *Electrochim. Acta*, **53**, 2386 (2008).
20. L. Cao, F. Xu, Y. Y. Liang, and H. L. Li, *Adv. Mater. (Weinheim, Ger.)*, **16**, 1853 (2004).
21. W. J. Zhou, J. Zhang, T. Xue, D. D. Zhao, and H. L. Li, *J. Mater. Chem.*, **18**, 905 (2008).
22. V. Gupta, T. Kusahara, H. Toyama, S. Gupta, and N. Miura, *Electrochem. Commun.*, **9**, 2315 (2007).
23. S. L. Chou, J. Z. Wang, H. K. Liu, and S. X. Dou, *J. Power Sources*, **182**, 359 (2008).
24. H. C. Liu and S. K. Yen, *J. Power Sources*, **166**, 478 (2007).
25. K. E. Heusler, *Encyclopedia of Electrochemistry of the Elements*, A. J. Bard, Editor, Vol. 3, Chap. 2, Marcel Dekker, New York (1973).
26. E. Frackowiak and F. Beguin, *Carbon*, **39**, 937 (2001).
27. R. Boggio, A. Carugati, and S. Trasatti, *J. Appl. Electrochem.*, **17**, 828 (1987); F. Svegl, B. Orel, M. G. Hutchins, and K. Kalcher, *J. Electrochem. Soc.*, **143**, 1532 (1996).
28. J. Gamby, P. L. Taberna, P. Simon, J. F. Fauvarque, and M. Chesneau, *J. Power Sources*, **101**, 109 (2001).
29. P. Kurzweil and H. J. Fischle, *J. Power Sources*, **127**, 331 (2004).
30. A. Hamelin, T. Vitanov, E. Sevastyanov, and A. Popov, *J. Electroanal. Chem. Interfacial Electrochem.*, **145**, 225 (1983).
31. S. L. Chou, F. Y. Cheng, and J. Chen, *J. Power Sources*, **162**, 727 (2006).